

Biometry reference range of the corpus callosum in neonates

An observational study

Yanyan Gao, MD^a, Kai Yan, MD^b, Lin Yang, MD, PhD^{c,*}, Guoqiang Cheng, MD, PhD^{b,*},
Wenhao Zhou, MD, PhD^b

Abstract

This study aims to present the reference range of corpus callosum by ultrasound imaging in neonates and to develop a clinically feasible screening method for congenital abnormalities of corpus callosum.

An observational study was conducted between January 2015 and July 2016; 2D and 3D ultrasound evaluations were conducted and virtual organ computer-aided analysis was applied in the volume calculation of corpus callosum. The following parameters were measured: thickness of the rostrum, thickness of the genu, thickness of the body, thickness of the splenium, anterior–posterior distance, true length of the corpus callosum and the volume of the corpus callosum. Inter- and intraobserver agreement was also evaluated. The corrected gestational age was between 38+0 and 47+2 weeks. The least-mean-square method was used to create the growth curve for each parameter.

Complete data sets were available in 317 neonates, ranging from 0 to 28 days of age. Reference values from the 1st to 99th percentiles were provided. All parameters showed a nonlinear growth trend with age. Inter- and intraobserver agreement was excellent for 2D and 3D parameters.

Our results suggested that computer techniques can assist in the volume assessment of corpus callosum. The 2D and 3D ultrasound data of 7 morphologic parameters may facilitate the identification of corpus callosum anomalies based on a large population.

Abbreviations: APD = anterior–posterior distance of corpus callosum, BT = thickness of the body of corpus callosum, CC = corpus callosum, CGA = corrected gestational age, CUS = cranial ultrasonography, GT = thickness of the genu of corpus callosum, LCC = true length of corpus callosum, LMS = least-mean-square method, RT = thickness of the rostrum of corpus callosum, ST = thickness of the splenium of corpus callosum, VCC = volume of corpus callosum, VOCAL = virtual organ computer-aided analysis.

Keywords: corpus callosum, neonates, ultrasound

1. Introduction

The corpus callosum (CC), which contains approximately 200 million axons, is the main commissure between the 2 cerebral hemispheres. Congenital abnormality of the CC is one of the most

common brain malformations in newborns. The prevalence of agenesis of the CC is 5/10,000 in the general population and 230–600/10,000 in neurodevelopmentally disabled children. These patients may suffer from varying degrees of mental, behavioral, and social impairments.^[1] The severity of the symptoms is mainly correlated with the type of CC anomaly. For instance, the neurodevelopmental outcome depends on which part of the CC is abnormal^[2] or whether the CC anomaly is isolated or syndromic.^[1] In addition, whether appropriate treatment and subsequent training are initiated in time may also significantly impact the prognosis.

Early identification of CC anomalies is crucial for a better prognosis.^[3] As an easy and nonradioactive imaging tool, ultrasonography has been routinely used in prenatal screening for malformations. It is highly sensitive in the detection of CC anomalies in fetuses.^[4] Nevertheless, this technique can lead to misdiagnoses as it is difficult to display a standard midsagittal plane, especially when the fetus is not in a proper position. In a recent study by Koning et al,^[5] the success rate reportedly ranged between 61% and 75% for the measurement of CC length in fetuses. The authors also conducted cranial ultrasonography (CUS) in the same cohort after birth; the success rate was 97%, which was much higher than that obtained during prenatal assessment.

CUS has been increasingly used in neonatal units over the past decades because of its distinct advantage in detecting special cranial disorders. In neonates, the anterior fontanelles are not closed, thus providing the acoustic window for scanning the midline brain structures.^[6] Recent advantages in 3D imaging

Editor: Vasile Valeriu Lupu.

YG and KY equally contributed to this study.

Competing Financial Interests statement: All the authors declare that there are no competing financial interests.

This research was supported by the National Natural Science Foundation of China (81471484, 81501289) and Science and Technology Commission of Shanghai Municipality (15XD1500800).

The authors have no conflicts of interest to disclose.

^a Ultrasonography Unit, ^b Department of Neonatology, ^c Clinical Genetic Center, Children's Hospital of Fudan University, Shanghai, China.

* Correspondence: Guoqiang Cheng, Department of Neonatology, Children's Hospital of Fudan University, Shanghai 201102, China (e-mail: gqchengcm@163.com), Lin Yang, Clinical Genetic Center, Children's Hospital of Fudan University, Shanghai 201102, China (e-mail: yanglin_fudan@163.com).

Copyright © 2018 the Author(s). Published by Wolters Kluwer Health, Inc. This is an open access article distributed under the Creative Commons Attribution-NoDerivatives License 4.0, which allows for redistribution, commercial and non-commercial, as long as it is passed along unchanged and in whole, with credit to the author.

Medicine (2018) 97:24(e11071)

Received: 27 November 2017 / Accepted: 16 May 2018

<http://dx.doi.org/10.1097/MD.00000000000011071>

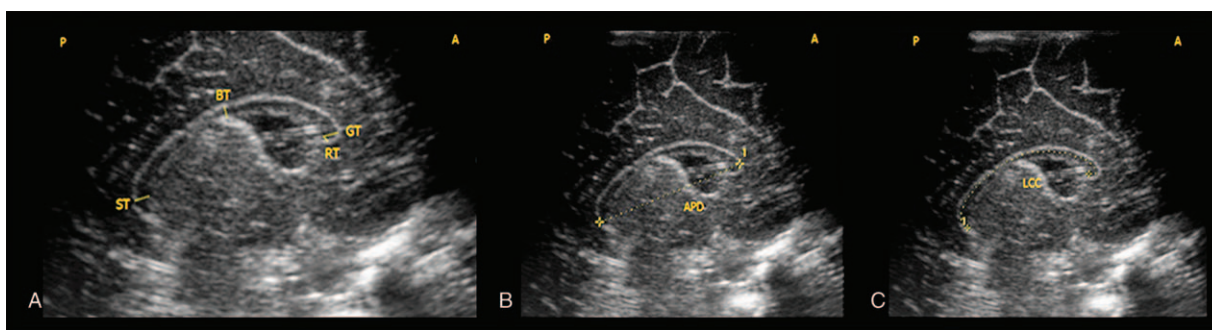


Figure 1. Descriptions of the 2D morphologic parameters. (A) Measurements of the RT, GT, BT, and ST, the thickness measured at the level of the rostum, genu, body and splenium. (B) Measurement of the APD, the distance between the anterior and posterior aspect of corpus callosum. (C) Measurement of the LCC, the curvilinear length from the starting point of the rostum to the ending point of the splenium at mid-thickness of corpus callosum. APD = anterior–posterior distance, BT = body thickness, GT = genu thickness, LCC = true length of corpus callosum, RT = rostum thickness, ST = splenium thickness.

techniques have also facilitated measurement and analysis (e.g., volume estimation) of certain structures of human bodies, allowing precise morphologic evaluation of organs.^[7,8] In this sense, establishment of a screening program for CC morphology in neonates will probably promote early detection of CC anomalies. However, the lack of present knowledge on CC morphology in neonates has become a major obstacle in development of this method. To the best of our understanding, there are few data on biometric reference values of the CC in neonatal period.

Therefore, this study sought to investigate the morphologic changes of the CC in normal Chinese newborns using ultrasonic imaging and 3D sonography. Based on corrected gestational week, biometric reference data of the CC were also provided.

2. Materials and methods

2.1. Study design

This is a cross-sectional study. Neonates between 1 and 28 days old were recruited from outpatient and inpatient departments in the Children's Hospital of Fudan University. All neonates studied were term-born (gestational age of more than 37 weeks), with a birth weight appropriate for gestational age. An appropriate-for-gestational age neonate should weigh between the 10th and the 90th percentiles for age. Exclusion criteria included congenital malformations, neurologic disorders, or metabolic diseases. The recruitment period was January 2015 to July 2016, and the study was approved by the Institutional Ethics Committee of Children's Hospital of Fudan University. The sample size was determined by the statistical calculation relating to estimation accuracy according to Jennen-Steinmetz and Wellek.^[9]

2.2. Imaging technique and measurement

All scans were performed by an experienced investigator, using the GE Voluson Expert 730 Ultrasound System, with a volumetric probe (RNA 5-9MH). When cranial ultrasound examinations were performed, neonates were placed in the supine position with the neck in neutral position, and sedation was provided by a pacifier when necessary. The midsagittal view was obtained through the acoustic window of the anterior fontanelle, and according to Achiron et al,^[10] the standard

midsagittal plane should include the corpus callosum, the cavem pellucidi, the fourth ventricle, and the cerebellar vermis in the same view. The gain and depth of the ultrasound system were adjusted to get the optimized image.

Following the image optimization, 2D measurements were obtained including thickness of the rostum (RT), thickness of the genu (GT), thickness of the body (BT), thickness of the splenium (ST), anterior–posterior distance (APD), and true length of the corpus callosum (LCC). The whole procedure took a mean of 2.5 minutes (1.6–3.1 minutes) for each patient. The above morphologic parameters are illustrated in Figure 1.

After 2D measurements were taken, the real-time 3D switch was activated, and the box was positioned over the region of interest, which included the whole contour of the corpus callosum. A sweep angle of 50° and the highest quality were set. After 3D scanning, images in three orthogonal planes (axial, sagittal and coronal) were displayed. The virtual organ computer-aided analysis (VOCAL) mode was used to evaluate the volume of the corpus callosum per the following protocol: first, the sagittal plane was chosen as the reference plane; second, the 3D image was rotated along the z-axis, and a rotation angle of 15° was selected so that the contour was manually delineated in 11 consecutive planes; finally, the volume of the corpus callosum (VCC) was calculated automatically by the computer. The entire procedure was performed off-line and took a mean of 10 minutes (7.8–13.1 minutes) for each patient. The manual delineation in the 11 consecutive planes is illustrated in Figure 2.

In case of imaging artifacts that may influence the measurements, cases were excluded from the study. All of the 2D and 3D measurements were repeated 3 times, and the mean values were used for statistical analysis.

To evaluate the intraobserver reliability, measurements were repeated 3 times every 2 weeks by 1 radiologist on a sample of 30 randomly selected neonates; the interobserver agreement was evaluated by 2 radiologists using the same sample; each radiologist was unaware of the results obtained by the other. 2D and 3D measurements were evaluated separately.

2.3. Statistical analysis

Corrected gestational age (CGA) was obtained by adding the gestational age and postnatal age. The least-mean-square method (LMS) was applied to construct the growth curve of the corpus callosum in neonates by weeks of CGA. The RT, GT, BT, ST,

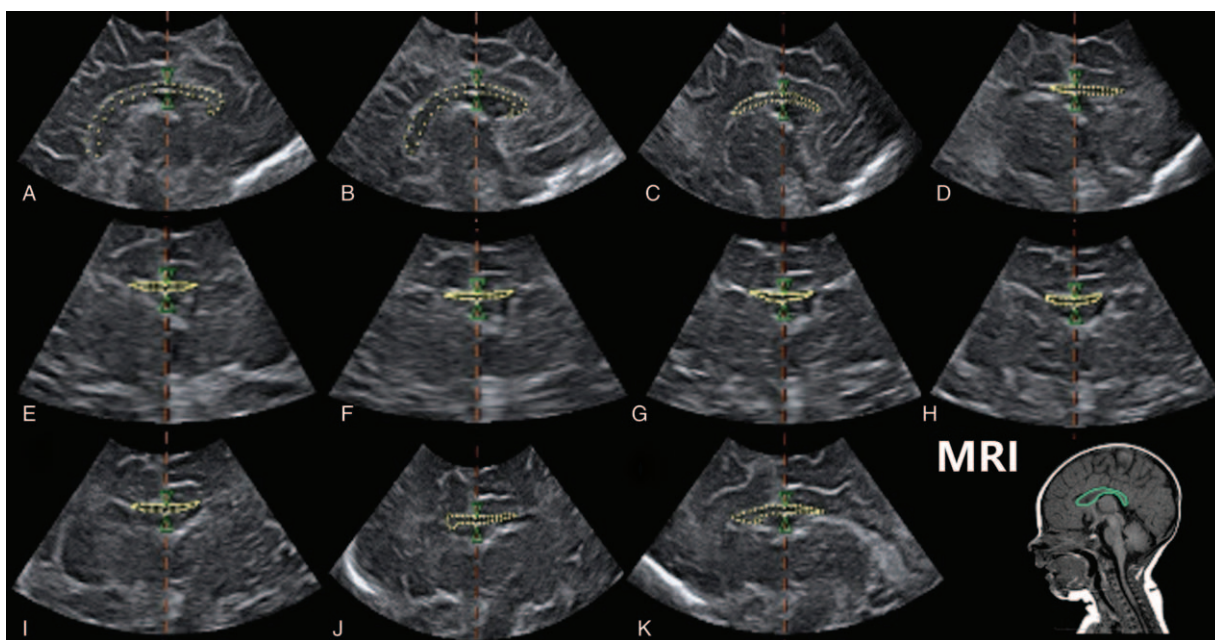


Figure 2. Using the manual contour method of the virtual organ computer-aided analysis, outer borders were delineated on a fixed axis with 15° rotations in 11 planes.

LPD, LCC, and VCC were presented as the 1st, 5th, 10th, 25th, 50th, 75th, 90th, 95th, and 99th percentiles, respectively, for each period of CGA. To assess the relationships between each morphologic parameter and the corrected gestational ages, as well as the relationship between the 2D parameters and the 3D ultrasound volumes, we used the Pearson correlation coefficient (*r*) analysis. One-way analysis of variance and *t*-test were used to assess the difference of intra- and interobserver, respectively.^[11] Statistical analyses were performed using Stata 12.0 SE (Stata, College Station, TX), the *P* value < .05 was considered statistically significant.

3. Results

Around 445 term-born neonates were initially recruited. A total of 17 cases were excluded for congenital malformations (7 for craniofacial dysostosis, 6 for cleft lip and palate, 4 for polydactyly), 48 cases were excluded for neurologic disorders (12 for birth asphyxia, 12 for meningitis, 9 for hydrocephalus, 7 for intraventricular hemorrhage>2, 5 for cerebral infarction, 3 for seizure attacks), 42 cases were excluded for metabolic diseases (15 for hypoglycemia, 10 for hypothyroidism, 10 for hypotonia, 5 for hyperglycemia, 2 for phenylketonuria). Artifacts with different degrees occurred in some images, so 21 these neonates were also excluded to ensure the accuracy of measurements. Thus, a total of 317 neonates were enrolled, including 148 girls and 169 boys. The study population was depicted in Figure 3. The gestational age was more than 37 weeks, and the CGA was between 38+0 and 47+2 weeks. The distribution of the number of children as a function of age is described in Table 1.

For the intraobserver reliability evaluation, *P* value was .35 for 2D measurement, .69 for 3D measurement. For the interobserver

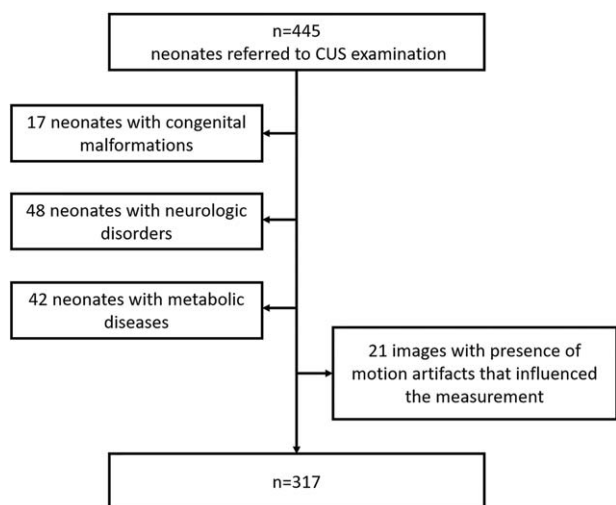


Figure 3. Flow diagram of patient selection. CUS examination=cranial ultrasound examination.

Table 1

Distribution of the number of neonates.

CGA, weeks	Number
38–38+6	23
39–39+6	30
40–40+6	51
41–41+6	60
42–42+6	38
43–43+6	32
44–44+6	29
45–45+6	21
46–46+6	15
47–47+2	18

CGA = corrected gestational age.

Table 2

Pearson correlation coefficient (*r*) analysis between each morphologic parameter and the corrected gestational age.

Morphologic parameter	<i>r</i> (CGA)	<i>P</i>
RT	0.3428	.014
GT	0.4848	<.001
BT	0.4641	<.001
ST	0.5038	<.001
APD	0.6599	<.001
LCC	0.6438	<.001
VCC	0.7065	<.001

APD = anterior–posterior distance, BT = body thickness, CGA = corrected gestational age, GT = genu thickness, LCC = true length of corpus callosum, RT = rostrum thickness, ST = splenium thickness, VCC = volume of corpus callosum.

agreement evaluation, *P* value was .59 for 2D measurement, and .66 for 3D measurement. The above results indicated good intra- and interobserver reliability and agreement.

By Pearson correlation analysis, morphologic parameters were correlated to CGA, and 2D measurements (RT, GT, BT, ST, APD, and LCC) were correlated to 3D measurement (VCC). Moderate agreement was found for GT, BT and ST to CGA ($P < .001$, $0.40 < r \leq 0.60$); good agreement was found for APD, LCC and VCC to CGA ($P < .001$, $0.60 < r \leq 0.80$); moderate agreement was found for GT, BT, ST and APD to VCC ($P < .001$, $0.40 < r \leq 0.60$); good agreement was found for LCC to VCC ($P < .001$, $0.60 < r \leq 0.80$) (for details see Tables 2 and 3).

A 3D model of the corpus callosum, constructed by the VOCAL method, is shown in Figure 4. The shape was displayed in a spatial form by rotating along three orthogonal axes. Reference values (from the 1st to the 99th percentiles) are provided for each morphological parameter in Table 4 and

Table 3

Pearson correlation coefficient (*r*) analysis between 2D parameter and 3D ultrasound volume.

2D parameter	<i>r</i> (VCC)	<i>P</i>
RT	0.3682	<.001
GT	0.4932	<.001
BT	0.5054	<.001
ST	0.5214	<.001
APD	0.5586	<.001
LCC	0.6433	<.001

APD = anterior–posterior distance, BT = body thickness, GT = genu thickness, LCC = true length of corpus callosum, RT = rostrum thickness, ST = splenium thickness, VCC = volume of corpus callosum.

depicted in Figure 5. All parameters showed a nonlinear growth trend from the CGA of 38+0 weeks to 47+2 weeks.

4. Discussion

In the present study, we utilized 3D ultrasound imaging and VOCAL methods to construct a model of the CC and evaluate the volume that, when combined with 2D measurements, could be used to assess the CC morphology in a more comprehensive way. To the best of our knowledge, this is the first time that morphologic reference values of the CC in term-born neonates were provided. For the neonates with a congenital CC anomaly, if detected at birth, they may have a chance to receive effective and targeted treatment and intervention as early as possible. CC anomalies could be isolated or complicated, with multiple congenital malformations or metabolic disorders, so we excluded the neonates with congenital malformations, neurologic disorders, or metabolic diseases from the study. We used the LMS



Figure 4. Corpus callosum model constructed by virtual organ computer-aided analysis, rotating along axial (A), coronal (B), and sagittal (C) axis, 3 orthogonal axes.

Table 4
Values from 1st to 99th percentiles for different parameters of corpus callosum.

CGA weeks	Percentile	RT, cm	GT, cm	BT, cm	ST, cm	APD, cm	LCC, cm	VCC, cm ³
38-38+6	1	0.07	0.26	0.14	0.27	3.84	5	0.976
	5	0.07	0.26	0.14	0.27	3.84	5	0.976
	10	0.08	0.27	0.15	0.28	3.94	5.01	1.151
	25	0.1	0.33	0.16	0.29	4.11	5.18	1.179
	50	0.11	0.37	0.19	0.35	4.23	5.3	1.333
	75	0.12	0.4	0.2	0.38	4.33	5.66	1.421
	90	0.13	0.46	0.21	0.43	4.62	5.76	1.547
	95	0.15	0.5	0.27	0.44	4.65	5.81	1.67
	99	0.15	0.5	0.27	0.44	4.65	5.81	1.67
39-39+6	1	0.08	0.25	0.13	0.23	4	5.38	1.005
	5	0.08	0.26	0.14	0.23	4	5.39	1.02
	10	0.08	0.28	0.16	0.24	4.06	5.43	1.065
	25	0.09	0.33	0.17	0.29	4.24	5.55	1.157
	50	0.12	0.39	0.2	0.33	4.38	5.7	1.331
	75	0.13	0.43	0.22	0.37	4.45	5.87	1.502
	90	0.14	0.45	0.23	0.43	4.67	6.03	1.571
	95	0.16	0.48	0.24	0.44	4.7	6.07	1.66
	99	0.17	0.51	0.24	0.44	4.71	6.08	1.68
40-40+6	1	0.07	0.26	0.14	0.23	3.94	4.91	0.776
	5	0.08	0.27	0.15	0.24	4.03	5.12	0.842
	10	0.08	0.29	0.17	0.26	4.16	5.27	0.931
	25	0.09	0.33	0.18	0.28	4.27	5.58	1.095
	50	0.1	0.38	0.2	0.33	4.44	5.77	1.284
	75	0.11	0.42	0.23	0.37	4.6	6.01	1.45
	90	0.12	0.47	0.25	0.44	4.73	6.22	1.556
	95	0.12	0.49	0.26	0.45	4.84	6.38	1.661
	99	0.12	0.49	0.26	0.46	4.85	6.48	1.738
41-41+6	1	0.09	0.26	0.15	0.2	3.96	5.17	0.857
	5	0.09	0.28	0.17	0.23	4.06	5.35	0.954
	10	0.09	0.31	0.17	0.26	4.11	5.48	1.02
	25	0.1	0.35	0.19	0.29	4.26	5.7	1.167
	50	0.11	0.39	0.21	0.33	4.48	5.91	1.337
	75	0.12	0.44	0.22	0.4	4.59	6.04	1.476
	90	0.13	0.47	0.24	0.44	4.75	6.19	1.579
	95	0.14	0.47	0.25	0.47	4.78	6.38	1.635
	99	0.14	0.48	0.26	0.49	4.81	6.45	1.77
42-42+6	1	0.08	0.29	0.15	0.18	4.19	5.33	1
	5	0.09	0.3	0.15	0.22	4.19	5.39	1.045
	10	0.09	0.32	0.16	0.24	4.22	5.61	1.152
	25	0.1	0.38	0.19	0.3	4.4	5.81	1.321
	50	0.11	0.4	0.2	0.37	4.59	6.04	1.488
	75	0.12	0.44	0.23	0.46	4.72	6.19	1.643
	90	0.15	0.48	0.25	0.48	4.8	6.37	1.883
	95	0.15	0.51	0.26	0.5	4.82	6.4	1.958
	99	0.15	0.52	0.26	0.53	4.85	6.43	1.986
43-43+6	1	0.08	0.31	0.17	0.31	4.22	5.52	1.132
	5	0.08	0.33	0.17	0.33	4.26	5.54	1.144
	10	0.08	0.35	0.18	0.37	4.35	5.71	1.197
	25	0.1	0.38	0.2	0.37	4.45	5.91	1.418
	50	0.12	0.42	0.23	0.44	4.56	6.13	1.573
	75	0.13	0.46	0.26	0.49	4.75	6.23	1.789
	90	0.14	0.48	0.28	0.53	4.8	6.44	2.001
	95	0.15	0.51	0.29	0.55	4.84	6.53	2.092
	99	0.15	0.53	0.29	0.57	4.84	6.56	2.169
44-44+6	1	0.08	0.29	0.15	0.27	4.18	5.22	1.01
	5	0.08	0.3	0.15	0.28	4.18	5.29	1.013
	10	0.09	0.33	0.18	0.32	4.23	5.52	1.058
	25	0.1	0.38	0.19	0.42	4.35	5.84	1.37
	50	0.12	0.42	0.23	0.48	4.6	6.17	1.865
	75	0.13	0.46	0.24	0.51	4.75	6.33	2.058
	90	0.14	0.51	0.26	0.57	4.94	6.51	2.213
	95	0.15	0.53	0.29	0.59	5.01	6.82	2.344
	99	0.15	0.53	0.29	0.59	5.01	6.97	2.344

(continued)

Table 4
(continued).

CGA weeks	Percentile	RT, cm	GT, cm	BT, cm	ST, cm	APD, cm	LCC, cm	VCC, cm ³
45–45+6	1	0.09	0.33	0.19	0.31	4.25	5.61	0.895
	5	0.09	0.33	0.19	0.31	4.25	5.61	0.895
	10	0.09	0.34	0.2	0.32	4.38	5.74	1.1
	25	0.103	0.4	0.22	0.45	4.49	6	1.348
	50	0.11	0.44	0.23	0.47	4.64	6.23	1.745
	75	0.12	0.48	0.24	0.53	4.87	6.56	2.031
	90	0.15	0.51	0.26	0.56	5.02	6.94	2.205
	95	0.15	0.55	0.26	0.6	5.02	6.96	2.261
	99	0.15	0.55	0.26	0.6	5.02	6.96	2.261
46–46+6	1	0.11	0.35	0.2	0.34	4.26	5.91	1.262
	5	0.11	0.35	0.2	0.34	4.26	5.91	1.262
	10	0.11	0.35	0.2	0.34	4.26	5.91	1.262
	25	0.11	0.42	0.22	0.41	4.41	5.94	1.409
	50	0.13	0.47	0.24	0.47	4.48	5.99	1.66
	75	0.13	0.48	0.25	0.53	4.58	6.16	1.821
	90	0.13	0.49	0.26	0.55	4.79	6.21	1.886
	95	0.13	0.49	0.26	0.55	4.79	6.21	1.886
	99	0.13	0.49	0.26	0.55	4.79	6.21	1.886
47–47+2	1	0.1	0.38	0.2	0.35	4.42	5.75	1.831
	5	0.1	0.38	0.2	0.35	4.42	5.75	1.831
	10	0.1	0.39	0.2	0.37	4.45	5.81	1.843
	25	0.1	0.46	0.21	0.44	4.6	6.24	1.903
	50	0.11	0.47	0.22	0.48	4.72	6.3	2.136
	75	0.12	0.52	0.26	0.53	4.97	6.86	2.368
	90	0.13	0.57	0.28	0.6	5	6.98	2.558
	95	0.13	0.57	0.29	0.6	5	7	2.582
	99	0.13	0.57	0.29	0.6	5	7	2.582

APD = anterior–posterior distance, BT = body thickness, CGA = corrected gestational age, GT = genu thickness, LCC = true length of corpus callosum, RT = rostrum thickness, ST = splenium thickness, VCC = volume of corpus callosum.

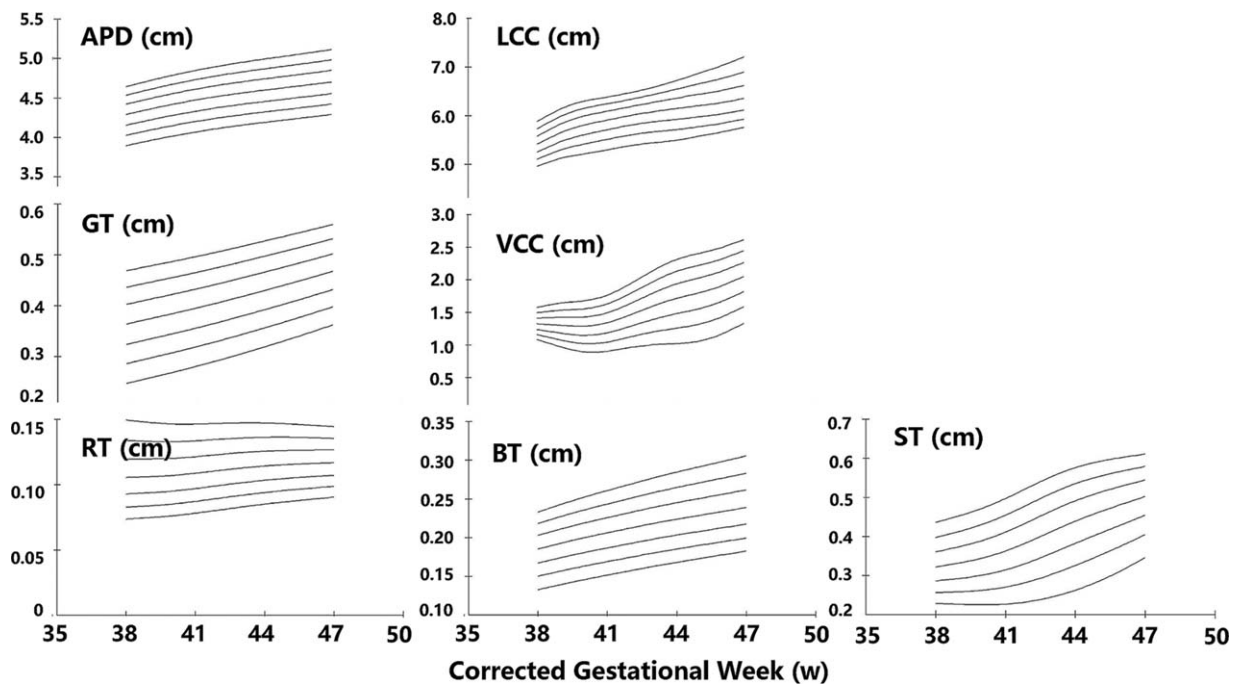


Figure 5. Reference ranges (1st, 5th, 10th, 50th, 90th, 95th, and 99th) for different morphologic parameters of corpus callosum. RT = rostrum thickness, GT = genu thickness, BT = body thickness, ST = splenium thickness, APD = anterior–posterior distance, LCC = true length of corpus callosum, VCC = volume of corpus callosum.

method that has been widely used for establishing growth curves in various studies.^[12,13] To enhance the precision, all of the 2D and 3D measurements were repeated 3 times, and the mean values were used for statistical analysis.

The CC is the largest white matter tract in the human brain. It is a late-maturing structure, consisting of approximately 2% to 3% of all cortical fibers. The principal function of the CC is the coordination and transfer of information between the 2 cerebral hemispheres.^[14] It is important for the integration of visuomotor, motor, and sensory function. Congenital structural abnormalities include agenesis and hypoplasia of the CC. Agenesis refers to total or partial absence and is visibly apparent; in contrast, hypoplasia refers to a thinner or shorter CC that has a normal-looking shape, thus making the reference values necessary for identification of the abnormality. Ultrasonography is most widely used for the imaging of the CC. As a non-radioactive, convenient, real-time technology, ultrasound imaging is suitable for serial measurements and can be applied in daily practice. Review of the perinatal literature provided biometric reference data of the CC in fetuses.^[15,16] There are, to the best of our knowledge, few publications on CC morphologic reference data for neonates. Koning et al^[5] combined fetal and neonatal ultrasonography markers for the CC into a single cohort and created a continuum for monitoring brain growth. Results from Koning et al confirmed the feasibility and reliability of cranial ultrasonography, while their attempt was to bridge the gap between prenatal and cranial ultrasonography, only one morphological parameter of CC was evaluated in their study. Recently, Klebermass-Schrehof et al^[2] conducted 3D ultrasound for CC in preterm infants with a gestational age <32 weeks and correlated the measurement data with neurodevelopmental outcome at 5 years of age, more significantly, they also found the correlation between different parts of CC and the outcome. Indeed, the significance of establishing reference data for CC in neonates not only lies in making up the weakness of prenatal ultrasonography but also in providing an accurate and easy screening method for detecting congenital callosal anomalies and evaluating neurodevelopment in early life.

The division of the region of the CC is not the same in all of the literature. Although controversial, it may be summarized as follows: traditional 4 regions defined as the rostrum, the genu, the body and the splenium, or six regions in which the body is divided into anterior, middle, and posterior segments. On the basis of anatomical division, several authors have used different methods to estimate CC morphology. As in our study, measurements were always acquired on a midsagittal view. According to some researchers, the CC is divided into 3, 4, or 6 subregions; thicknesses were measured for each subregion. Others have also measured the anterior–posterior distance or the true length of CC.^[2,3,17,18] The more regions measured, the more detailed morphologic information potentially acquired, but the drawback is that more-region methods often need to be based on an array of distance-dividing tools and are not all easy to use in daily practice. In our study, we favored the 4-region method, in which the landmarks used for measurements were relatively easy to distinguish. Once a midsagittal view is obtained, it takes less than 4 minutes to gather all 6 of the 2D measurements.

While studies on term-born neonatal CC morphology have not been published before, our results are in line with previous studies conducted on the nonlinear growth trend in fetuses and in the value of the reference. Pashaj et al^[19] established reference values of the CC from 17–41 weeks GA in fetuses. When the reference ranges for 37–39+6 and 40–41 weeks GA in the study by Pashaj were compared with ours for the same CGA, the values were

consistent with each other. The same is true when a comparison is made between our results and those of Garel et al,^[15] who established the morphologic reference values by MRI imaging from birth to 15 years. In the future, the reliability of our data could be further confirmed in a larger sample.

There is a high individual variation in the morphology of the CC. It may appear tubular, due to absent or slight narrowing at the level of the body, or it may be bulbous, with a marked widening of the splenium.^[20] The high variability accounts for possible difficulties in determining CC size by simple 2D measurements; 3D ultrasonography can evaluate the organ in a multiplanar way and calculate the volume, allowing identification of subtle changes in size. In previous studies, the VOCAL method had been used for prenatal US in irregular-shaped organs, such as the kidneys and lungs, to predict intrauterine growth restriction.^[7,8] The accuracy of the VOCAL method has been confirmed to be similar to multiplanar methods.^[21] This is the first time the VOCAL method is being used in CC volume estimation. In our procedure, manual traces of 11 different planes of the CC take less than 10 minutes, and the volume can be calculated automatically. The CC model construction looked similar, in morphology, to the dissection. Additionally, the Pearson correlation coefficient (*r*) analysis showed a statistical significance for the relationship between 2D parameters and 3D ultrasound volume, indicating that the volume could also be used as a reliable parameter in CC morphology estimation, compensating for the shortcomings of 2D assessment.

The insight into the function of the CC emerged from research on patients who had a therapeutic resection of the CC; a subsequent series of studies on white brain matter revealed the association between abnormalities of the CC and a spectrum of neuropsychiatric disorders including autism, schizophrenia, and Alzheimer's disease.^[22–25] In recent years, developments in sequencing technology have recognized that genetic factors contribute to callosal abnormality in the vast majority of cases.^[26] More than 200 genes associated with CC anomaly have been listed in the Online Mendelian Inheritance in Man (OMIM) database (accessed March 2017). A great concern has arisen regarding whether CC anomalies could be linked to special clinical statuses. However, specific knowledge is lacking, in that CC anomalies are likely to be misdiagnosed due to the shortcomings of the present detection methods; for prenatal examination, the success rate is limited due to fetal position, and for ascertainment after birth, neuroimaging is not undertaken without the presence or suspicion of a serious condition; thus, the asymptomatic or mildly affected cases may have no opportunity for further examination. Our assumption is that, based on a reliable reference range, a neonatal screening protocol for CC anomalies could be embedded in routine CUS examinations, facilitating the identification of CC anomalies. Based on a large population, we hope that this approach will be helpful in exploring the mechanism of CC anomalies, and to improve the treatment and prognosis.

There are some considerations that should be taken into account. First, the present study was conducted in a tertiary children's hospital; most neonates enrolled in the study were brought to the hospital for minor neonatal conditions, such as mild jaundice or upper respiratory tract infection. Although the minor disorders are not indicative of any neurodevelopmental diseases, we still need more medical centers join into the study of to establish CC reference curve representative of the general population. Second, in the present study, the operations were performed by an experienced investigator, who is skilled in ultrasound imaging and measurements, which may lead to a

shorter procedure time, compared to freshmen. Therefore, to validate replication of the data in our findings, it is necessary to combine the data collected in other maternal and child health centers and to enlarge the sample size by introducing the protocol to more neonatologists.

5. Conclusions

We have first constructed a 3D model of the CC and calculated the volume using the VOCAL method. Combined with the other 6 2D parameters, we have provided biometric data of the CC in cranial US imaging, during the neonatal period, and the data are reproducible and easy to use for screening. In the future, the use of the reference value will allow increased identification of congenital callosal anomalies through cranial US screening, make it possible to correlate CC biometry with the clinical status, and finally improve the treatment and prognosis of the disorders associated with CC abnormalities.

Acknowledgments

We thank all the neonates for their participants in the study.

Author contributions

Conceptualization: Yanyan Gao, Lin Yang, Guoqiang Cheng, Wenhao Zhou.

Data curation: Yanyan Gao.

Formal analysis: Kai Yan.

Funding acquisition: Wenhao Zhou.

Investigation: Wenhao Zhou.

Methodology: Yanyan Gao, Lin Yang.

Software: Kai Yan.

Supervision: Guoqiang Cheng.

Validation: Yanyan Gao.

Writing – original draft: Yanyan Gao.

Writing – review & editing: Yanyan Gao.

References

- [1] Palmer EE, Mowat D. Agenesis of the corpus callosum: a clinical approach to diagnosis. *Am J Med Genet C Semin Med Genet* 2014;166C:184–97.
- [2] Klebermass-Schrehof K, Aumuller S, Goeral K, et al. Biometry of the corpus callosum assessed by 3D ultrasound and its correlation to neurodevelopmental outcome in very low birth weight infants. *J Perinatol* 2017;37:448–53.
- [3] Nosarti C, Rushe TM, Woodruff PWR, et al. Corpus callosum size and very preterm birth: relationship to neuropsychological outcome. *Brain* 2004;127:2080–9.
- [4] Merz E. Targeted depiction of the fetal corpus callosum with 3D-ultrasound. *Ultraschall in Der Medizin* 2010;31:1441–1441.
- [5] Koning IV, Roelants JA, Groenenberg IAL, et al. New ultrasound measurements to bridge the gap between prenatal and neonatal brain growth assessment. *Am J Neuroradiol* 2017;38:1807–13.
- [6] van Wezel-Meijler G, Steggerda SJ, Leijser LM. Cranial ultrasonography in neonates: role and limitations. *Semin Perinatol* 2010;34:28–38.
- [7] Tedesco GD, Bussamra LCD, Araujo E, et al. Reference range of fetal renal volume by three-dimensional ultrasonography using the vocal method. *Fetal Diagn Ther* 2009;25:385–91.
- [8] Maged A, Youssef G, Hussien A, et al. The role of three-dimensional ultrasonography fetal lung volume measurement in the prediction of neonatal respiratory function outcome. *J Matern Fetal Neonatal Med* 2017;1–6. [Epub ahead of print].
- [9] Jennen-Steinmetz C, Wellek S. A new approach to sample size calculation for reference interval studies. *Stat Med* 2005;24:3199–212.
- [10] Achiron R, Kivilevitch Z, Lipitz S, et al. Development of the human fetal pons: in utero ultrasonographic study. *Ultrasound Obstet Gynecol* 2004;24:506–10.
- [11] Li YK, Pearce EC, Mainthia R, et al. Comparison of ventilation and voice outcomes between unilateral laryngeal pacing and unilateral cordotomy for the treatment of bilateral vocal fold paralysis. *ORL J Otorhinolaryngol Relat Spec* 2013;75:68–73.
- [12] Cole TJ, Statnikov Y, Santhakumaran S, et al. Birth weight and longitudinal growth in infants born below 32 weeks' gestation: a UK population study. *Arch Dis Child Fetal Neonatal Ed* 2014;99:F34–40.
- [13] Li Y. Electrical stimulation to promote selective reinnervation of denervated laryngeal muscles, Ph.D. dissertation, Vanderbilt University; 2016. (URN: etd-08102016-113705).
- [14] Griffiths PD, Batty R, Reeves MJ, et al. Imaging the corpus callosum, septum pellucidum and fornix in children: normal anatomy and variations of normality. *Neuroradiology* 2009;51:337–45.
- [15] Garel C, Cont I, Alberti C, et al. Biometry of the corpus callosum in children: MR imaging reference data. *AJNR Am J Neuroradiol* 2011;32:1436–43.
- [16] Bornstein E, Monteagudo A, Santos R, et al. A systematic technique using 3-dimensional ultrasound provides a simple and reproducible mode to evaluate the corpus callosum. *Am J Obstet Gynecol* 2010;202:24.
- [17] Suganthy J, Raghuram L, Antonisamy B, et al. Gender- and age-related differences in the morphology of the corpus callosum. *Clin Anat* 2003;16:396–403.
- [18] Habib M, Gayraud D, Oliva A, et al. Effects of handedness and sex on the morphology of the corpus callosum: a study with brain magnetic resonance imaging. *Brain Cogn* 1991;16:41–61.
- [19] Pashaj S, Merz E, Wellek S. Biometry of the fetal corpus callosum by three-dimensional ultrasound. *Ultrasound Obstet Gynecol* 2013;42:691–8.
- [20] Prendergast DM, Ardekani B, Ikuta T, et al. Age and sex effects on corpus callosum morphology across the lifespan. *Hum Brain Mapp* 2015;36:2691–702.
- [21] Raine-Fenning NJ, Clewes JS, Kendall NR, et al. The interobserver reliability and validity of volume calculation from three-dimensional ultrasound datasets in the in vitro setting. *Ultrasound Obstet Gynecol* 2003;21:283–91.
- [22] Aoki Y, Yoncheva YN, Chen B, et al. Association of white matter structure with autism spectrum disorder and attention-deficit/hyperactivity disorder. *JAMA Psychiatry* 2017;74:1120–8.
- [23] Takahashi M, Matsui M, Nakashima M, et al. Callosal size in first-episode schizophrenia patients with illness duration of less than one year: a cross-sectional MRI study. *Asian J Psychiatr* 2017;25:197–202.
- [24] Ardekani BA, Bachman AH, Figarsky K, et al. Corpus callosum shape changes in early Alzheimer's disease: an MRI study using the OASIS brain database. *Brain Struct Funct* 2014;219:343–52.
- [25] Li Y. To understand the brain—the 2016 annual meeting of society for neurosciences: a conference report. *Neural Regen Res* 2016;11:1912–3.
- [26] Hinkley LB, Marco EJ, Brown EG, et al. The contribution of the corpus callosum to language lateralization. *J Neurosci* 2016;36:4522–33.